Prestack migration velocity analysis: determination of interval velocities

Kamal Al-Yahya

ABSTRACT

The velocity analysis method presented in this paper uses iterative prestack migration. In each iteration, the field profiles are migrated with a velocity model and the error in the velocity model is estimated from the curvature of events in common receiver gathers. The velocity obtained from the curvature of an event is averaged over all depths above that event. The average velocities are used to estimate interval velocities which are constrained to exclude unreasonable velocity models. This sequence (migration, calculation of residual velocity, and updating the velocity model) is repeated until convergence is achieved. I processed field data using this method and obtained reasonable results after two iterations.

INTRODUCTION

This paper continues the discussion of velocity analysis by prestack migration. The principle of this scheme was first discussed in Al-Yahya and Muir (1984a). In Al-Yahya (1986a) I showed some synthetic examples and in the last SEP report (Al-Yahya, 1986b), I showed some preliminary field data results. In those examples I estimated the ratio of the average migration velocity to the average medium velocity as a function of depth. In this paper, I complete the process by computing the average medium velocity and subsequently the interval velocities. These interval velocities constitute the new model which can be used as the input to the next iteration.

REVIEW OF PRESTACK MIGRATION VELOCITY ANALYSIS

The velocity analysis method of this paper measures an entity called γ from the curvature of events (reflections or refractions) in common receiver gathers (CRG's). At the i-th depth step, γ is defined as

$$\gamma_i = \frac{(\bar{v}_m)_i}{\bar{v}_i} , \tag{1}$$

where v_m is the migration velocity, v is the medium velocity, and bars denotes averaging,

$$\bar{v}_i = \frac{\sum_{j=1}^{j=i} v_j}{i} \tag{2}$$

Note that, as mentioned in Al-Yahya and Muir (1984b), it is unfortunate that the curvature in the CRG's depends not only on γ but also on the structure. We therefore have to search for γ in all possible local dips. Rough limits on the dip in an area are normally known so the search is made within those limits.

The goal of the method presented in this paper is to drive all events towards $\gamma = 1$, namely $v_m = v$. This goal is achieved by iteratively changing the current velocity model and calculating γ's until the process converges. Note that in (1), γ is defined in terms of average velocities from which interval velocities need to be computed.

The method can thus be summarized as follows:

- Define an initial model
- Begin loop:
  - Migrate the profiles using the current velocity model.
  - Determine γ as a function of depth by measuring the curvature in migrated CRG's.
  - Compute average velocities from γ and the current velocity model.
  - Compute interval velocities from the average velocities.
  - If change in interval velocities is small, exit loop.
- End loop:

I will next describe computing interval velocities from average velocities.

COMPUTING INTERVAL VELOCITIES

Assuming the depth axis is sampled uniformly, the interval velocity at the i-th depth step is obtained from the average velocity as follows,

$$v_i = i\bar{v}_i - (i-1)\bar{v}_{i-1} \ , \tag{3}$$

where average velocities are obtained by using equation (1) after migration. One problem with equation (3) is that some γ's may belong to multiples or coherent noise and the average velocities they give will result in unreasonable values for the interval velocities. Another problem is the great sensitivity of obtaining interval velocities from average velocities which requires heavy damping to get a stable solution. These problems are similar to the problems of obtaining interval velocities from stacking velocities in conventional velocity analysis. To solve these problems in conventional velocity analysis, John Toldi (Toldi, 1985) proposed a method in which the model is perturbed using the gradient of an objective function. The gradient is calculated at the current model position and requires calculating the derivative of the objective function in the stacking-velocity space.

In Toldi's scheme, knowing the position of the model in the interval-velocity space implies knowing its position in the stacking-velocity space because the two spaces are related via the Dix equation. In the scheme presented in this paper, the space that I search is a residual-velocity space in which I don't know the current model position because knowing the residual velocities implies knowing the true velocities, signaling the end of the search! I therefore cannot compute a gradient direction and use a scheme that is similar to Toldi's. However, I can use the position of the peaks as a guide and try to be as close to them as possible given some constraints on the velocity model. The constraints that are imposed on the velocity model may include smoothness (especially in the lateral direction) and any available a priori information about the velocity. It is well known that sharp variations in velocities cannot be detected by integral methods, namely methods that use only travel time information (Stolt, 1986; Clærbout, 1985). Unnecessary velocity variations in the lateral direction create imaginary fault-plane reflections (Clærbout, 1985). It is therefore sensible to impose a smooth velocity function requirement.

The problem is therefore set up like this:
Let $\mathbf{v}'$ be the velocity vector implied by the picked γ's; let $\hat{\mathbf{v}}$ be an a priory velocity model vector used as a constraint (if desired); then find $\mathbf{v}$ that minimizes

$$E = \sum_{j=1}^{j=N} \left[\bar{v}_j(v_i) - \bar{v}'_j \right]^2 + \alpha \sum_{i=1}^{i=N} (v_i - v_{i-1})^2 + (v_i - v_{i+1})^2 + \beta \sum_{i=1}^{i=N} (v_i - \hat{v}_i)^2 \qquad (4)$$

where N is the number of depth steps, α and β are damping factors, and bars denote averaging. Taking the derivative with respect to v_i and noting that

$$\begin{aligned} \frac{\partial \bar{v}_j}{\partial v_i} &= \frac{1}{j} \quad \text{for} \quad j \geq i \ , \\ &= 0 \quad \text{for} \quad j < i \ , \end{aligned}$$

the problem reduces to solving this equation

$$\mathbf{Av} + \mathbf{Tri}(-\alpha, 2\alpha + \beta, -\alpha)\mathbf{v} = \mathbf{B}\bar{\mathbf{v}}' + \beta\hat{\mathbf{v}} \qquad (5)$$

where $\mathbf{A}$ is a matrix whose entries are

$$A_{ij} = \sum_{k=\max(i,j)}^{k=N} \frac{1}{k^2} \ ,$$

$\mathbf{B}$ is an upper triangular matrix whose entries are

$$\begin{aligned} B_{ij} &= \frac{1}{j} \quad \text{for} \quad j \geq i \\ &= 0 \quad \text{for} \quad j < i \ , \end{aligned}$$

and $\mathbf{Tri}$ is a tridiagonal matrix.

MUTING AND MIXING

Two ideas can be borrowed from conventional processing. First, if prestack migration is done by the hybrid method, in which time shifting is applied after downward continuation,

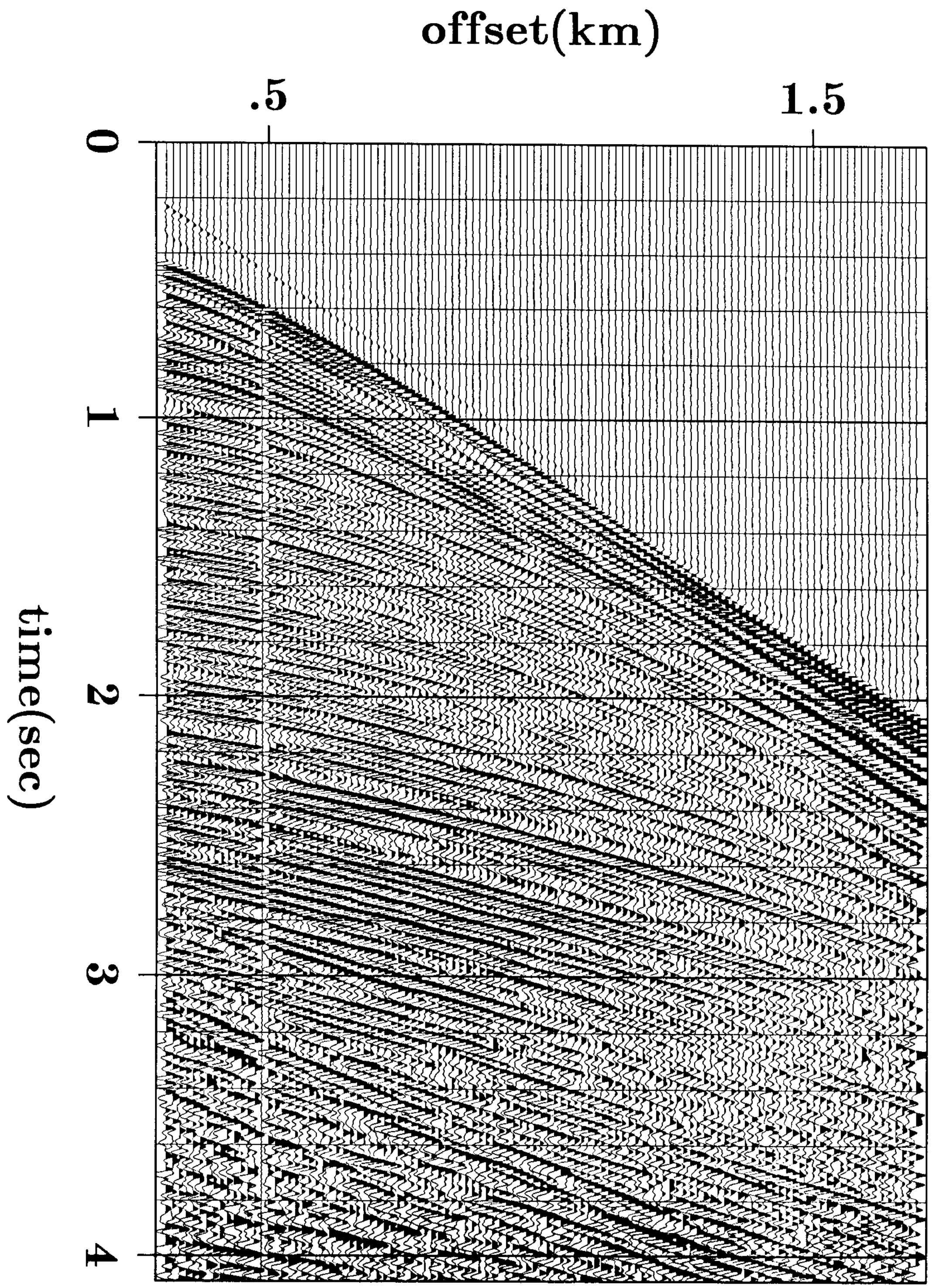

FIG. 1. A typical marine profile used for velocity analysis example.

a mute similar to NMO mute should be applied. Second, adjacent CRG's can be mixed to increase signal/noise ration (at the expense of resolution), just like mixing adjacent common mid-points.

A FIELD DATA EXAMPLE

The input to the velocity analysis scheme presented here is field profiles. I used marine profiles from the Gulf of Mexico. These profiles are well-sampled in the receiver axis (receiver spacing is 12.5 m), and have been sub-sampled in the shot axis (to make the receiver spacing 50 m). This arrangement is most suitable for profile processing in which the geophone axis is the critical one and need to be well-sampled while the shot axis need not be heavily sampled. A typical profile is shown in Figure 1. A total of 28 profile were used, each having 240 receivers.

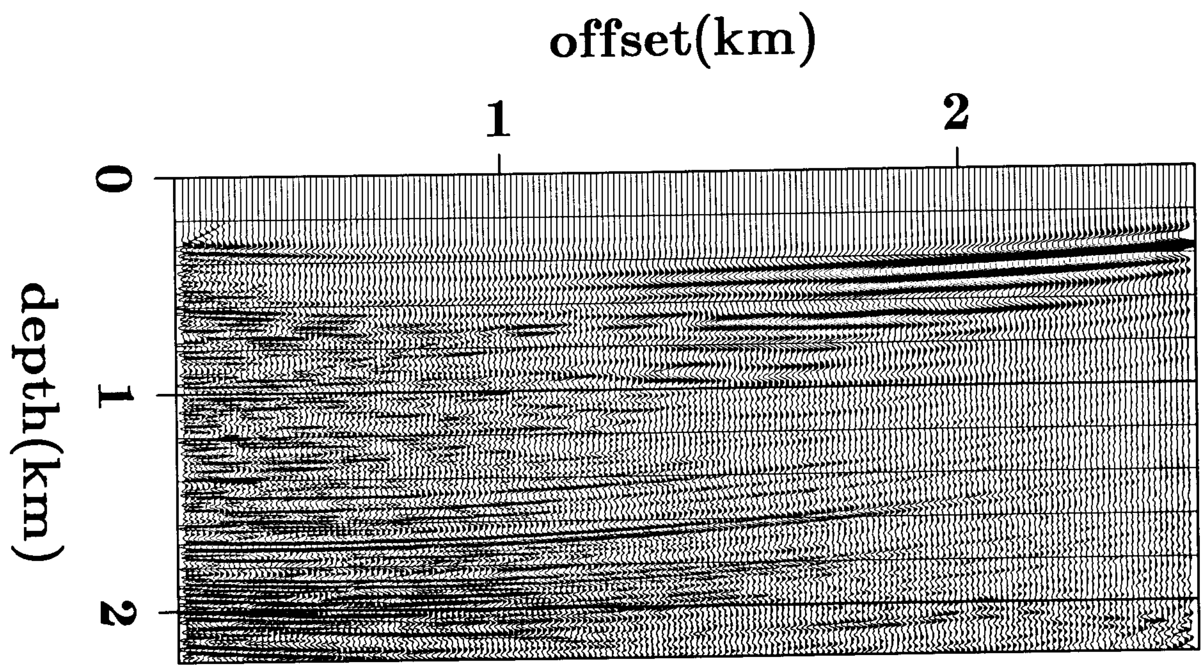

FIG. 2. The profile of Figure 1 after migration with water velocity. No mute was applied. Notice the dominant enenergy at wide offsets due to supercritical reflections.

The first step in the velocity analysis method of this paper is migrating all profiles with a velocity model. A model obtained by a rough conventional velocity analysis can serve as a starting model. In this example, I used a constant velocity model having the velocity of water (1.5 km/sec). Figure 2 shows the result of migrating the profile in Figure 1 with this velocity and Figure 3 shows the stacked section (obtained by summing along the shot axis). Because the velocity used in migration was not the same as the medium velocity, the migrated profiles and stacked section do not represent the geology of the subsurface.

The next step is to sort the data to produce common receiver gathers (CRG's). A

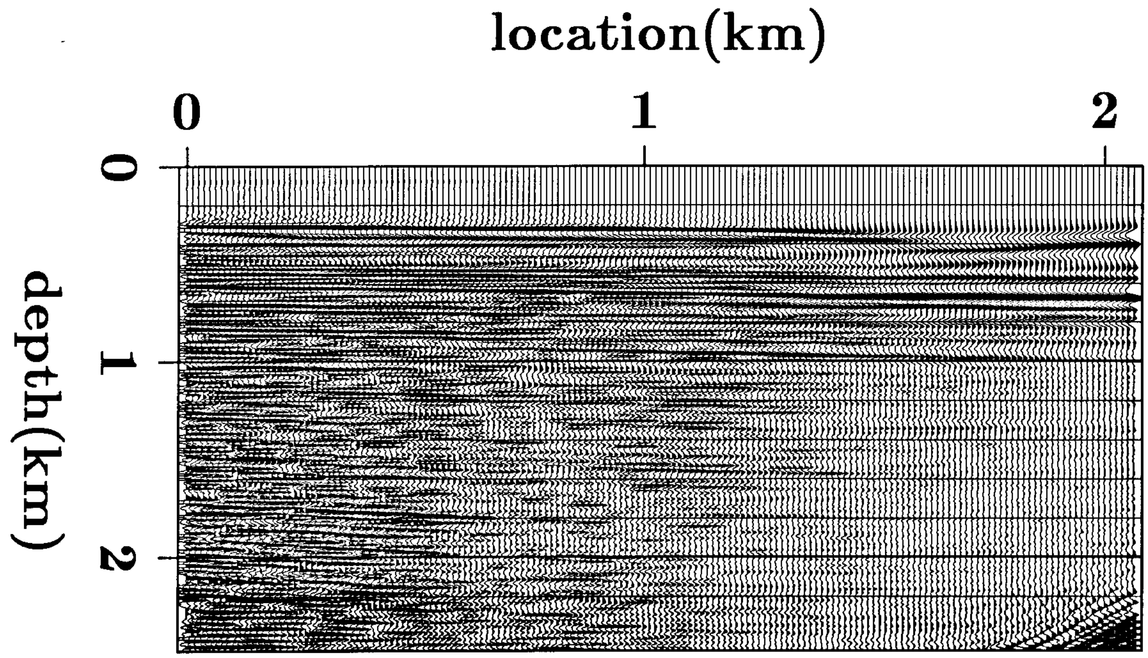

FIG. 3. The migrated and stacked image obtained by migrating and stacking the profiles with the water velocity.

typical CRG is shown in Figure 4a. Now we are ready to compute the velocity ratio γ from the observed curvature in these CRG's. For this example, because the geology does not appear to be complicated, I limited the search to zero dip. Figure 4b shows a semblance panel of the velocity ratio γ as a function of travel-time depth. As mentioned before, these γ's give average velocities from which the interval velocities need to be computed. Figure 5 shows the resulting interval velocity model which was constrained to be smooth.

Using the new velocity model in Figure 5, the profiles were migrated again. One such profile is shown in Figure 6 and the stacked section is shown in Figure 7. A typical CRG is shown in Figure 8, and the semblance of velocity ratio is shown in Figure 8. We see that using the new velocity model, most events are now close to $\gamma = 1$ meaning that the migration velocity is close to the medium velocity. However, some events deviate from $\gamma = 1$ so we may need to slightly modify the current velocity model.

Figure 9 shows the velocity model obtained from the semblance in Figure 8 (here again, smoothness constraints were used). A typical profile migrated with this model is shown in Figure 10 and the stacked section is shown in Figure 11. A CRG obtained from these profiles is shown in Figure 12a. From this CRG, we need to measure the curvature to see if events are horizontally aligned. Figure 12b shows the semblance panel for this CRG in which events are a little closer to $\gamma = 1$ than in Figure 8b.

We can continue the iterations until we are satisfied, but the velocity model is not expected to change significantly, because we have most of the events at $\gamma = 1$. Those events

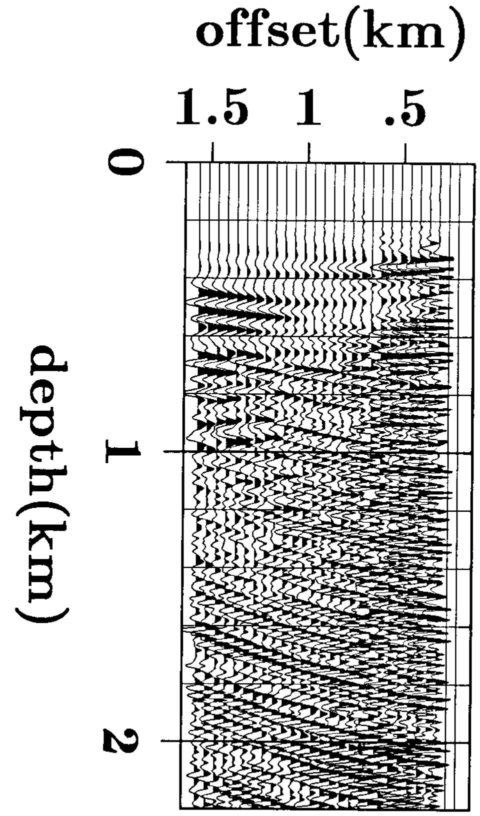

FIG. 4. a. A typical migrated CRG obtained from profiles migrated with the water velocity.

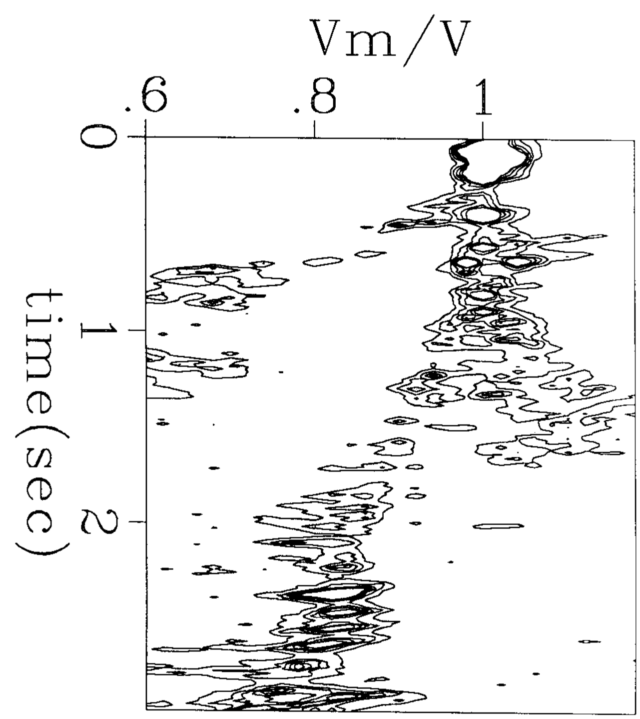

FIG. 4. b. A semblance panel showing the velocity ratio γ vs. travel-time depth.

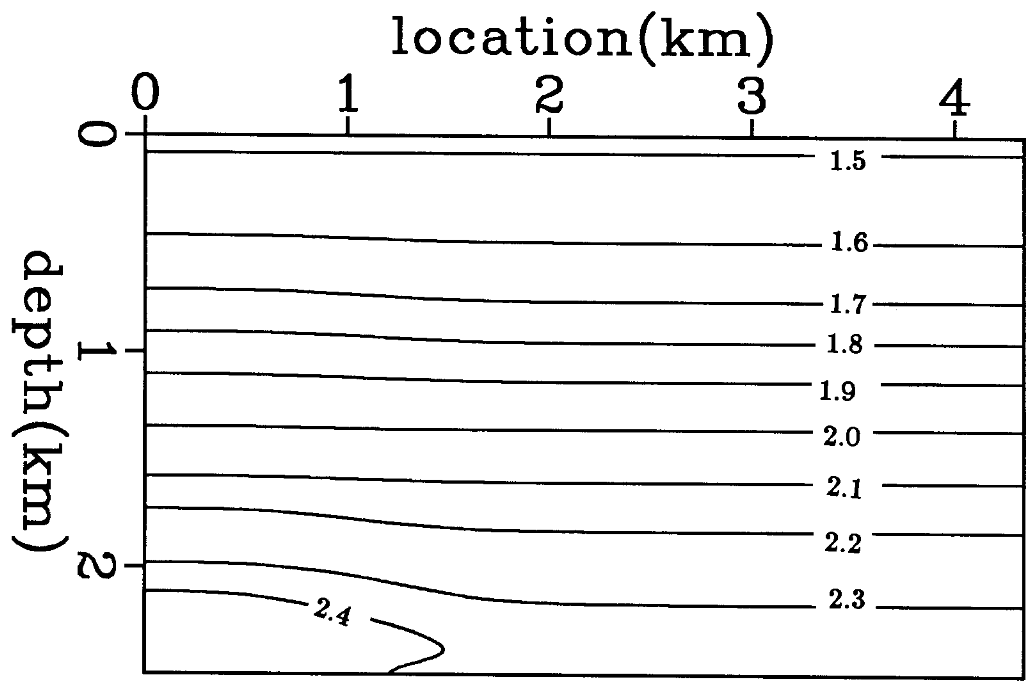

FIG. 5. A contour plot of the model obtained from the first iteration using the semblances in Figure 4. Contour labels are velocities in km/sec.

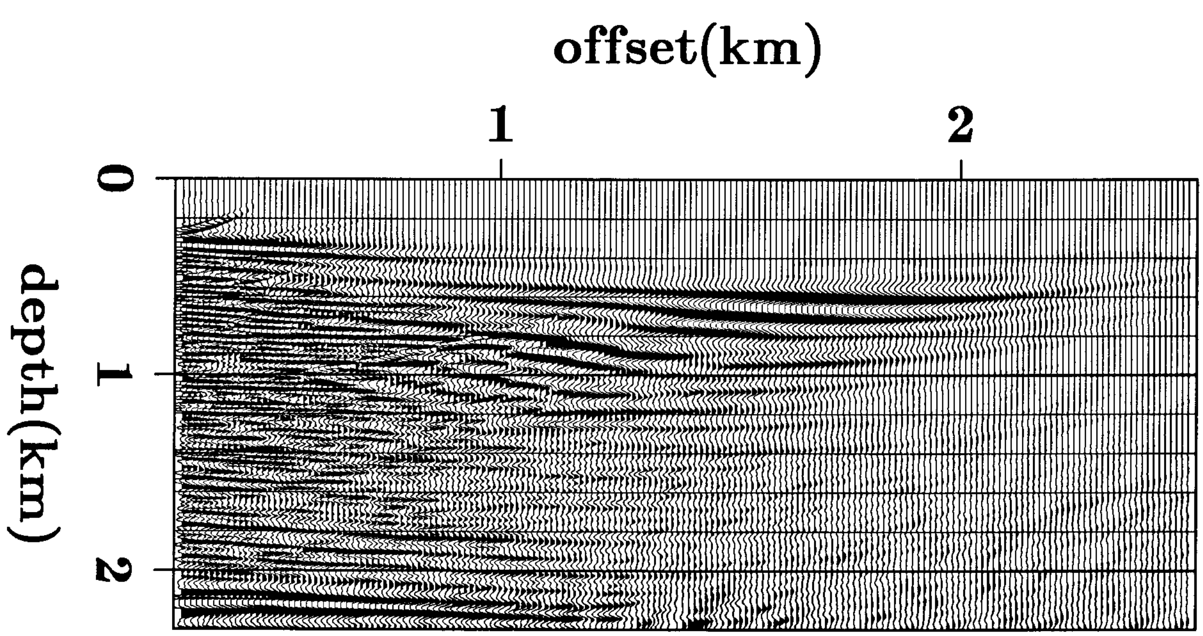

FIG. 6. The profile of Figure 1 after migration with the velocity model in Figure 5.

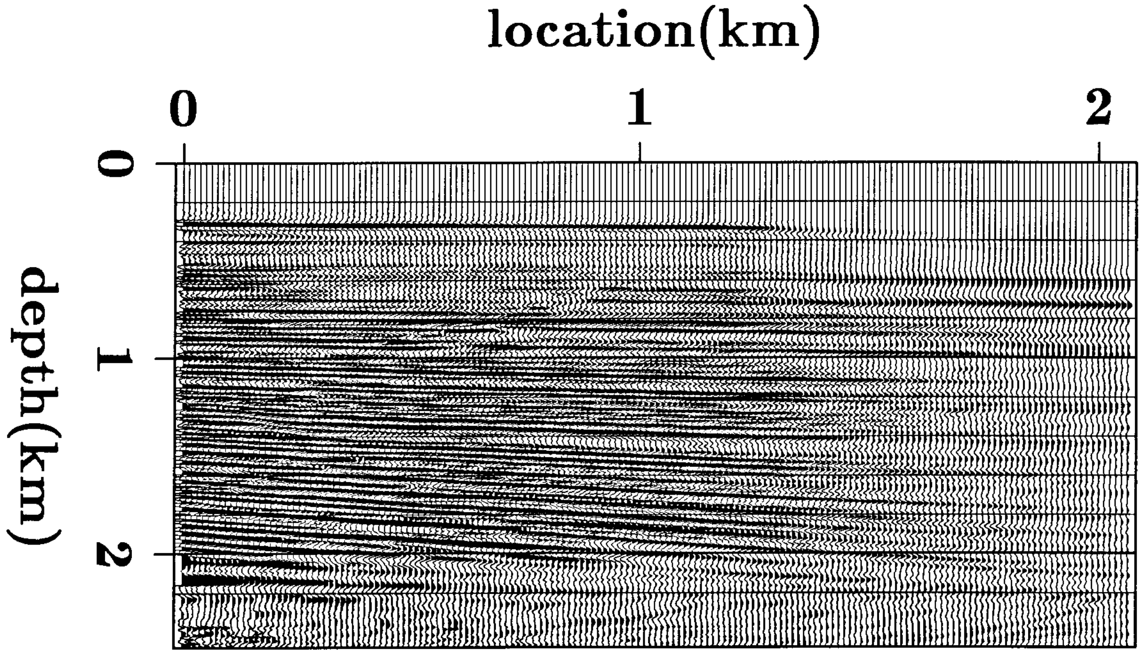

FIG. 7. The migrated and stacked image obtained by migrating and stacking the profiles with the model in Figure 5. Muting was applied to suppress wide angle reflections.

FIG. 8. a. A typical migrated CRG obtained from profiles migrated with the velocity model in Figure 5.

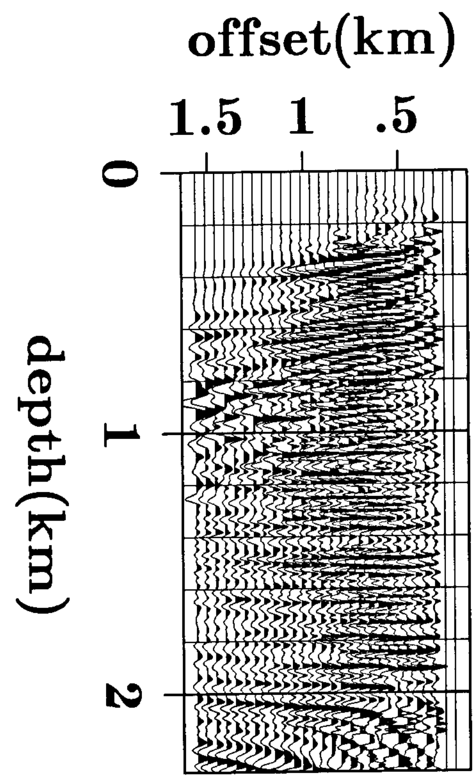

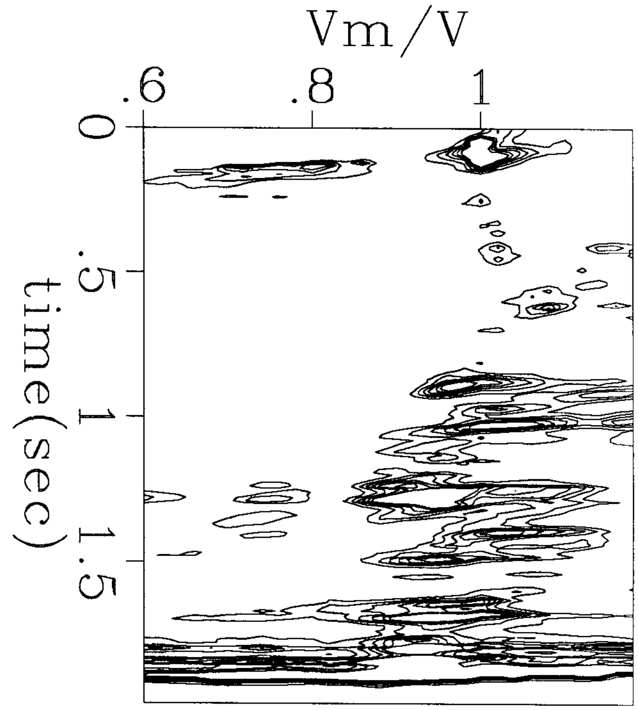

FIG. 8. b. A semblance panel showing the velocity ration γ vs. travel-time depth.

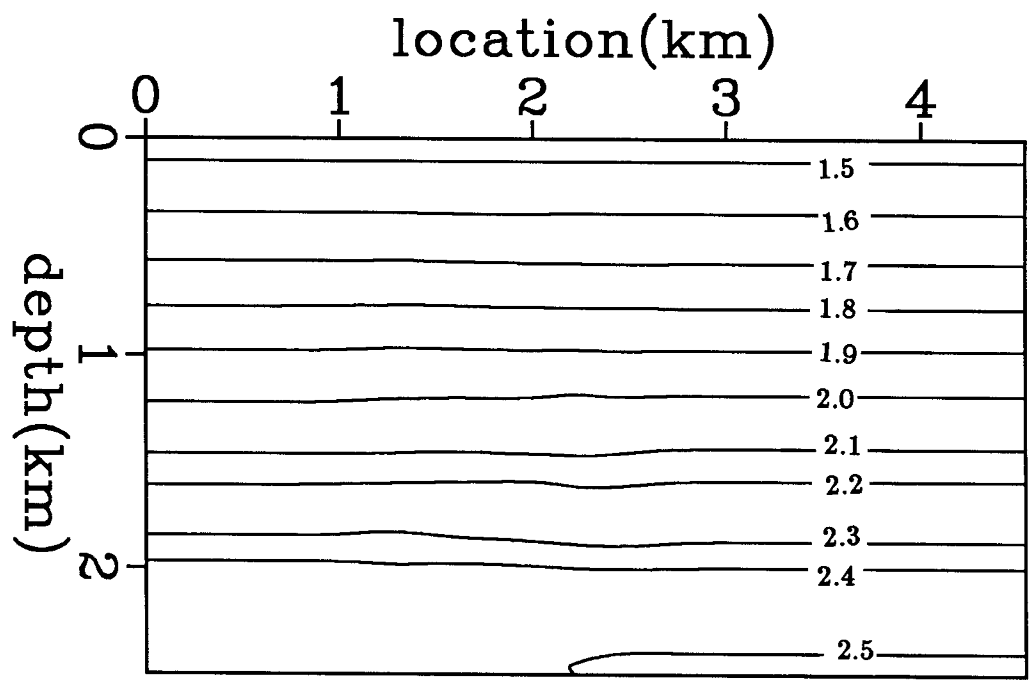

FIG. 9. A contour plot of the model obtained from the second iteration using the semblances in Figure 8. Contour labels are velocities in km/sec.

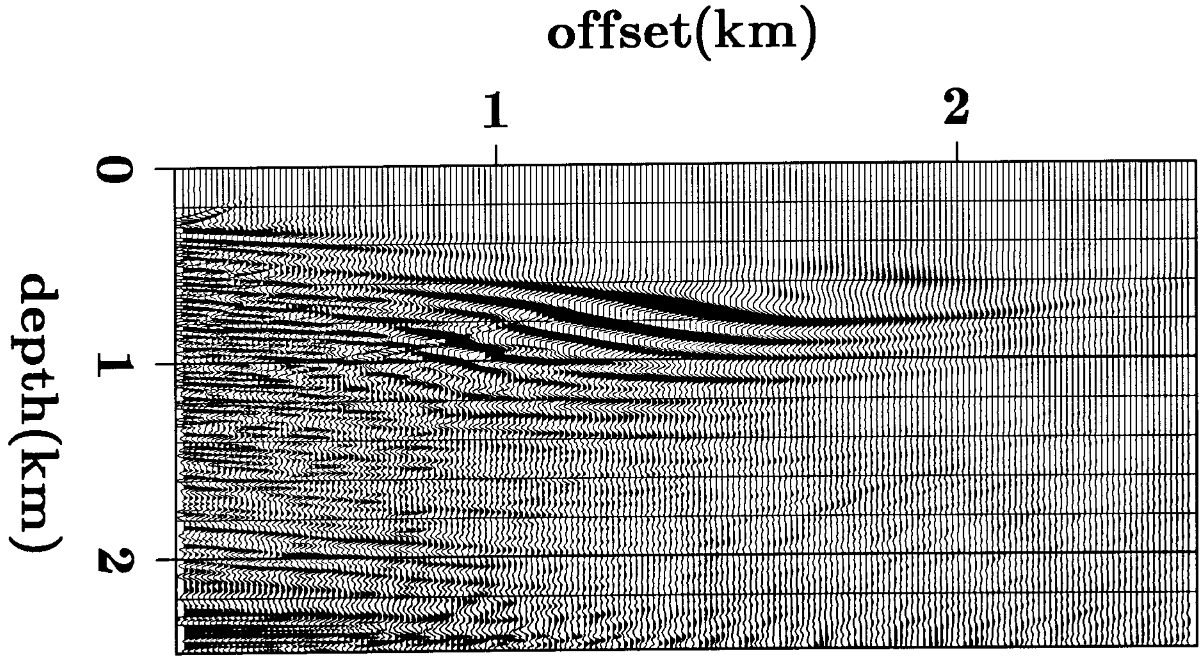

FIG. 10. The profile of Figure 1 after migration with the velocity model in Figure 9.

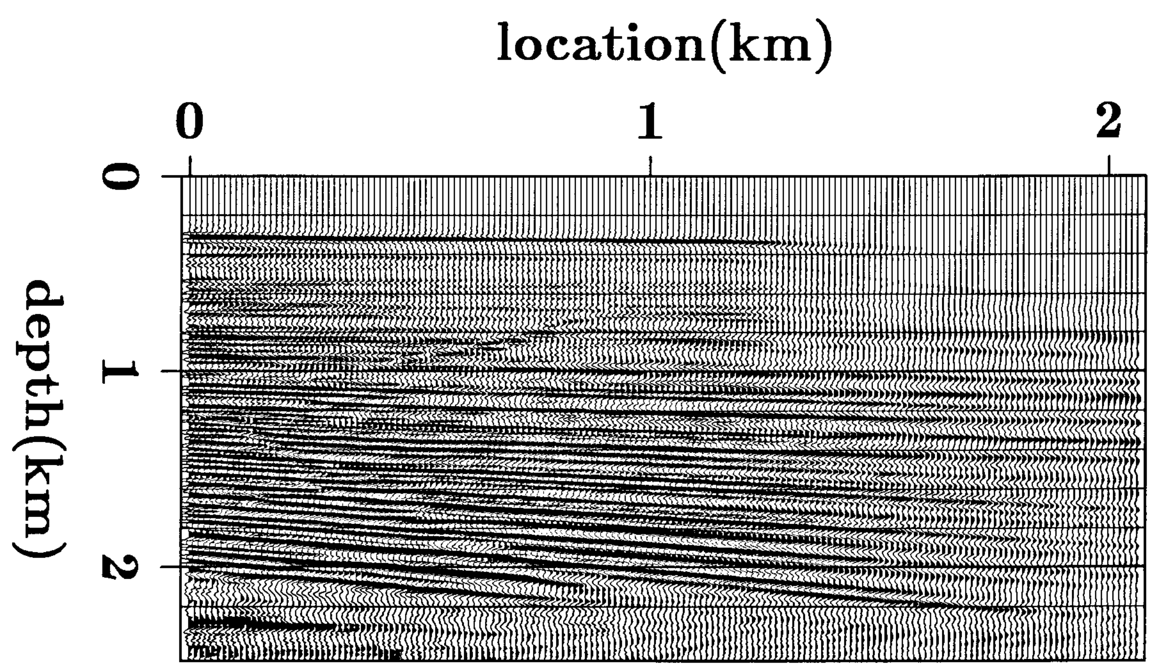

FIG. 11. The migrated and stacked image obtained by migrating and stacking the profiles with the model in Figure 9. Muting was applied to suppress wide angle reflections.

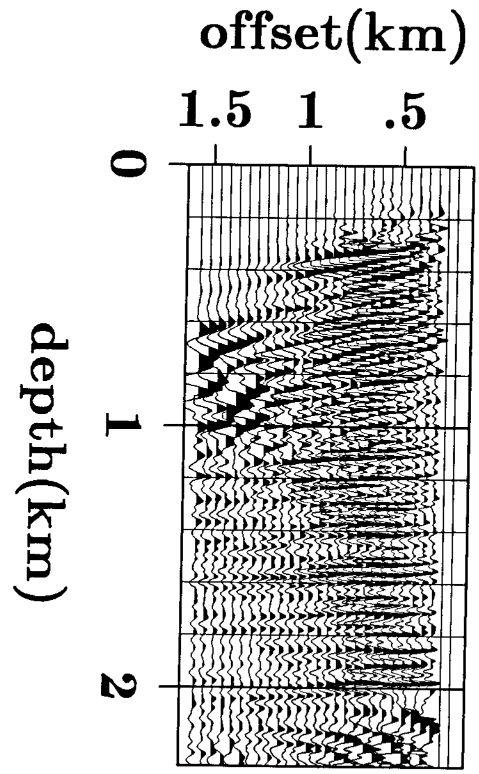

FIG. 12. a. A typical migrated CRG obtained from profiles migrated with the velocity model in Figure 9.

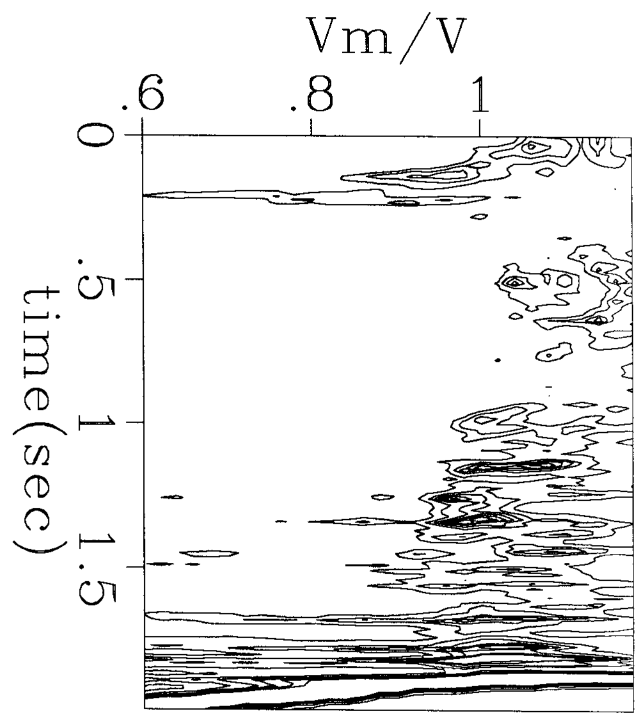

FIG. 12. b. A semblance panel showing the velocity ration γ vs. travel-time depth.

that are away from $\gamma = 1$ are probably multiples or coherent noise. I will therefore end this illustrative example at this point.

In summary, I started with a constant velocity model and estimated a new velocity model from the curvature in the migrated CRG's. I then re-migrated the data and estimated a new model. This process can be continued if it has not converged, but in the example I have shown, two iterations were enough. The final output is a velocity model and migrated profiles. The stacked and migrated section was obtained by summing along the shot axis. This stacked section has the high wavenumber information (the reflectivity) in a concise form that is helpful for geologic interpretation while the velocity model has the low wavenumber information. Migrated CRG's are also useful for interpretation, especially for studying the reflectivity variation with angle of incidence.

CONCLUSIONS

Prestack migration is a velocity indicator and can therefore be used in velocity analysis. The scheme presented in this paper uses an iterative approach; in each iteration the new interval velocities are computed from the average-velocity ratio, γ. It was necessary to impose some constraints on the updated model to exclude unreasonable models. The most important constraints are the smoothness of the model, especially in the lateral direction.

REFERENCES

Al-Yahya, K., and Muir, F., 1984a, Velocity analysis using prestack migration, SEP–38, p. 105-112.

—, 1984b, Velocity analysis using prestack migration: Applications, SEP–41, p. 121-147.

Al-Yahya, K., 1986a, Velocity analysis by prestack migration, SEP–48, p. 45-63.

—, 1986b, Migration velocity analysis of field data: preliminary results, SEP–50, p. 129-138.

Clærbout, J.F., 1985, Imaging the earth's interior, Blackwell Scientific Publication, p. 376-378.

Toldi, J.L., 1985, Velocity analysis without picking, Ph.D. thesis, Stanford University.

Stolt, R.H., and Benson, A.K., 1986, Seismic migration: theory and practice, Geophysical Press.

H. Kaufman, "*Velocity Functions in Seismic Prospecting*," *Geophysics*, XVIII, 2(1953), 289-297.

TABLE I

RELATIONS BASED ON A GIVEN INSTANTANEOUS-VELOCITY—DEPTH FUNCTION

Instantaneous-Velocity—Depth Function	Corresponding Average-Velocity—Depth Function	Corresponding Instantaneous-Velocity—Vertical-Time Function	Corresponding Average-Velocity—Vertical-Time Function	Travel Time from Shot-Point to any Point of Path
$v=v(z)$	$v_a=v_a(z)$	$v(t_v)$	$v_a=v_a(t_v)$	$t=t(\theta)$
$v_0(1+kz)^{1/n}$	$\frac{(n-1)kv_0}{n}\cdot\frac{z}{(1+kz)^{(n-1)/n}-1}$, $n\neq 1$	$v_0\left[1+\frac{(n-1)kv_0}{n}t_v\right]^{1/(n-1)}$, $n\neq 1$	$\frac{\left[\left(1+\frac{(n-1)kv_0}{n}t_v\right)^{n/(n-1)}-1\right]}{kt_v}$, $n\neq 1$	$\frac{n}{kv_0\sin^{n-1}\theta_0}\int_{\theta_0}^{\theta}\sin^{n-2}\theta\,d\theta$
$v_0(1+kz)$	$\frac{kv_0z}{\log(1+kz)}$	$v_0e^{kv_0t_v}$	$\frac{e^{kv_0t_v}-1}{kt_v}$	$\frac{1}{kv_0}\log\frac{\tan(\theta/2)}{\tan(\theta_0/2)}$
$v_0(1+kz)^{1/2}$	$\frac{v_0}{2}[(1+kz)^{1/2}+1]$	$v_0(1+\frac{1}{2}kv_0t_v)$	$v_0(1+\frac{1}{4}kv_0t_v)$	$\frac{2(\theta-\theta_0)}{kv_0\sin\theta_0}$
$v_0(1+kz)^{1/3}$	$\frac{2kv_0z}{3[(1+kz)^{2/3}-1]}$	$v_0(1+\frac{2}{3}kv_0t_v)^{1/2}$	$\frac{[(1+\frac{2}{3}kv_0t_v)^{3/2}-1]}{kt_v}$	$\frac{3(\cos\theta_0-\cos\theta)}{kv_0\sin^3\theta_0}$
$v_0+Az^{1/n}$	$\frac{A^nz}{n\int_{v_0}^{v}\frac{(v-v_0)^{n-1}}{v}dv}$	$t_v=\frac{n}{A^n}\int_{v_0}^{v}\frac{(v-v_0)^{n-1}}{v}dv$		$\frac{nv_0^{n-1}}{A^n\sin^{n-1}\theta_0}\int_{\theta_0}^{\theta}\frac{(\sin\theta-\sin\theta_0)^{n-1}}{\sin\theta}d\theta$
$v_0+Az^{1/2}$	$\frac{A^2z}{2\left[Az^{1/2}-v_0\log\left(1+\frac{Az^{1/2}}{v_0}\right)\right]}$	$t_v=\frac{2}{A^2}\left[v-v_0-v_0\log\frac{v}{v_0}\right]$		$\frac{2v_0}{A^2\sin\theta_0}\left[\theta-\theta_0-(\sin\theta_0)\log\frac{\tan(\theta/2)}{\tan(\theta_0/2)}\right]$
$Az^{1/n}$	$\frac{(n-1)}{n}Az^{1/n}$	$\left(\frac{n-1}{n}\cdot A^n\right)^{1/(n-1)}t_v^{1/(n-1)}$	$\left(\frac{(n-1)A}{n}\right)^{n/(n-1)}t_v^{1/(n-1)}$	$\frac{n}{A^np^{n-1}}\int_0^{\theta}\sin^{n-2}\theta\,d\theta$
v_0e^{kz}	$\frac{kv_0z}{1-e^{-kz}}$	$\frac{v_0}{1-kv_0t_v}$	$\frac{1}{kt_v}\log\frac{1}{1-kv_0t_v}$	$\frac{\sin\theta_0(\cot\theta_0-\cot\theta)}{kv_0}$
$v_1\tanh(Az+B)$	$\frac{Av_1z}{\log\frac{\sinh(Az+B)}{\sinh B}}$	$v_1(1+e^{-2Av_1t_v}\operatorname{cosech}^2B)^{-1/2}$	$\frac{1}{At_v}[\sinh^{-1}(e^{Av_1t_v}\sinh B)-B]$	$(Av_1)^{-1}(\beta^2\sin^2\theta_0-1)^{-1/2}\left[\tan^{-1}\frac{\cos\theta_0}{(\beta^2\sin^2\theta_0-1)^{1/2}}-\tan^{-1}\frac{\cos\theta}{(\beta^2\sin^2\theta_0-1)^{1/2}}\right]+\frac{1}{Av_1}(\tanh^{-1}\cos\theta_0-\tanh^{-1}\cos\theta)$, $\beta=\frac{v_1}{v_0}$
$v_1-\frac{A}{z+a}$	$\frac{v_1z}{z+\frac{A}{v_1}\log\left(1+\frac{\beta z}{a}\right)}$, $\beta=\frac{v_1}{v_0}$			$\frac{a(\beta-1)}{\beta^2v_0}\left\{\frac{\beta\sin\theta_0}{\beta^2\sin^2\theta_0-1}\left[\frac{\cos\theta_0}{(\beta-1)\sin\theta_0}-\frac{\cos\theta}{\beta\sin\theta_0-\sin\theta}\right]+\frac{2\beta^2\sin^2\theta_0-1}{(\beta^2\sin^2\theta_0-1)^{3/2}}\left[\sin^{-1}\left(\frac{\beta\sin\theta_0\sin\theta-1}{\beta\sin\theta_0-\sin\theta}\right)-\sin^{-1}\left(\frac{\beta\sin^2\theta_0-1}{(\beta-1)\sin\theta_0}\right)\right]+\log\frac{\tan(\theta/2)}{\tan(\theta_0/2)}\right\}$, $\beta=\frac{v_1}{v_0}$
$v_1\left(1-\frac{z^2}{z_1^2}\right)^{-1/2}$	$\frac{2v_1z_1z}{z(z_1^2-z^2)^{1/2}+z_1^2\sin^{-1}(z/z_1)}$			$\frac{z_1\sin^2\theta_0}{v_0}\left\{\frac{1}{2}\cot\theta(\cot^2\theta_0-\cot^2\theta)^{1/2}+(1+\frac{1}{2}\cot^2\theta_0)\left[\frac{\pi}{2}-\sin^{-1}\left(\frac{\cot\theta}{\cot\theta_0}\right)\right]\right\}$
$v_0(1+A^2z^2)^{1/2}$	$\frac{Av_0z}{\sinh^{-1}Az}$	$v_0\cosh Av_0t_v$	$\frac{1}{t_v}\sinh Av_0t_v$	$\frac{1}{Av_0}[K(\cos\theta_0)-F(\psi,\cos\theta_0)]$, $\psi=\sin^{-1}(\sec\theta_0\cos\theta)$
$A\left(\frac{z}{z+h}\right)^{1/2}$	$\frac{Az}{[z(z+h)]^{1/2}+h\tanh^{-1}\left(\frac{z}{z+h}\right)^{1/2}}$			$\frac{hp\sin\theta\cos\theta}{(p^2A^2-\sin^2\theta)(1-p^2A^2)}+\frac{h(2p^2A^2-1)}{2A(p^2A^2-1)^{3/2}}\left[\frac{\pi}{2}-\sin^{-1}\left(\frac{p^2A^2-(2p^2A^2-1)\sin^2\theta}{p^2A^2-\sin^2\theta}\right)\right]$
$v_0\cosh Az$	$\frac{v_0Az}{\tan^{-1}(\sinh Az)}$	$v_0\sec v_0At_v$	$\frac{1}{At_v}\sinh^{-1}(\tan v_0At_v)$	$\frac{1}{Av_0}\left[\frac{\pi}{2}-\tan^{-1}\left(\frac{\sin\theta_0\cos\theta}{(\cos^2\theta_0-\cos^2\theta)^{1/2}}\right)\right]$

Instantaneous-Velocity—Depth Function	Displacement	Vertical Depth to any Point of Path	Depth—Vertical-Time Function	Surface-to-Surface Travel Time	Range	Depth to Maximum Penetration
$v=v(z)$	$x=x(\theta)$	$z=z(\theta)$	$z=z(t_v)$	T	X	Z
$v_0(1+kz)^{1/n}$	$\frac{n}{k\sin^n\theta_0}\int_{\theta_0}^{\theta}\sin^n\theta\,d\theta$	$\frac{1}{k}\left(\frac{\sin^n\theta}{\sin^n\theta_0}-1\right)$	$\frac{1}{k}\left[\left(1+\frac{(n-1)kv_0}{n}t_v\right)^{n/(n-1)}-1\right]$, $n\neq 1$	$\frac{2n}{kv_0\sin^{n-1}\theta_0}\int_{\theta_0}^{\pi/2}\sin^{n-2}\theta\,d\theta$	$\frac{2n}{k\sin^n\theta_0}\int_{\theta_0}^{\pi/2}\sin^n\theta\,d\theta$	$\frac{1}{k}(\csc^n\theta_0-1)$
$v_0(1+kz)$	$\frac{\cos\theta_0-\cos\theta}{k\sin\theta_0}$	$\frac{1}{k}\left(\frac{\sin\theta}{\sin\theta_0}-1\right)$	$\frac{1}{k}(e^{kv_0t_v}-1)$	$\frac{2}{kv_0}\log\cot(\theta_0/2)$	$\frac{2\cot\theta_0}{k}$	$\frac{1}{k}(\csc\theta_0-1)$
$v_0(1+kz)^{1/2}$	$\frac{1}{2k\sin^2\theta_0}[(2\theta-\sin 2\theta)-(2\theta_0-\sin 2\theta_0)]$	$\frac{1}{k}\left(\frac{\sin^2\theta}{\sin^2\theta_0}-1\right)$	$v_0t_v(1+\frac{1}{4}kv_0t_v)$	$\frac{4}{kv_0\sin\theta_0}\left(\frac{\pi}{2}-\theta_0\right)$	$\frac{1}{k\sin^2\theta_0}(\pi-2\theta_0+\sin 2\theta_0)$	$\frac{1}{k}\cot^2\theta_0$
$v_0(1+kz)^{1/3}$	$\frac{3}{k\sin^3\theta_0}[(\cos\theta_0-\cos\theta)-\frac{1}{3}(\cos^3\theta_0-\cos^3\theta)]$	$\frac{1}{k}\left(\frac{\sin^3\theta}{\sin^3\theta_0}-1\right)$	$\frac{1}{k}[(1+\frac{2}{3}kv_0t_v)^{3/2}-1]$	$\frac{6\cos\theta_0}{kv_0\sin^3\theta_0}$	$\frac{6}{k\sin^3\theta_0}(\cos\theta_0-\frac{1}{3}\cos^3\theta_0)$	$\frac{1}{k}(\csc^3\theta_0-1)$
$v_0+Az^{1/n}$	$\frac{nv_0^n}{A^n\sin^n\theta_0}\int_{\theta_0}^{\theta}\sin\theta(\sin\theta-\sin\theta_0)^{n-1}d\theta$	$\left[\frac{v_0(\sin\theta-\sin\theta_0)}{A\sin\theta_0}\right]^n$		$\frac{2nv_0^{n-1}}{A^n\sin^{n-1}\theta_0}\int_{\theta_0}^{\pi/2}\frac{(\sin\theta-\sin\theta_0)^{n-1}}{\sin\theta}d\theta$	$\frac{2nv_0^n}{A^n\sin^n\theta_0}\int_{\theta_0}^{\pi/2}\sin\theta(\sin\theta-\sin\theta_0)^{n-1}d\theta$	$\left[\frac{v_0}{A}(\csc\theta_0-1)\right]^n$
$v_0+Az^{1/2}$	$\frac{v_0^2}{A^2\sin^2\theta_0}[\theta-\theta_0+2\sin\theta_0\cos\theta-\frac{1}{2}(\sin 2\theta+\sin 2\theta_0)]$	$\left[\frac{v_0(\sin\theta-\sin\theta_0)}{A\sin\theta_0}\right]^2$	$t_v=\frac{2}{A^2}\left[Az^{1/2}-v_0\log\left(1+\frac{Az^{1/2}}{v_0}\right)\right]$	$\frac{4v_0}{A^2\sin\theta_0}\left[\frac{\pi}{2}-\theta_0-(\sin\theta_0)\log\cot\frac{\theta_0}{2}\right]$	$\frac{v_0^2}{A^2\sin^2\theta_0}(\pi-2\theta_0-\sin 2\theta_0)$	$\left[\frac{v_0}{A}(\csc\theta_0-1)\right]^2$
$Az^{1/n}$	$\frac{n}{A^np^n}\int_0^{\theta}\sin^n\theta\,d\theta$	$\frac{\sin^n\theta}{A^np^n}$	$\left(\frac{n-1}{n}\cdot At_v\right)^{n/(n-1)}$	$\frac{n\pi^{1/2}}{A^np^{n-1}}\frac{\Gamma\left(\frac{n-1}{2}\right)}{\Gamma\left(\frac{n}{2}\right)}$	$\frac{n\pi^{1/2}}{A^np^n}\frac{\Gamma\left(\frac{n+1}{2}\right)}{\Gamma\left(\frac{n}{2}+1\right)}$	$\frac{1}{A^np^n}$
v_0e^{kz}	$\frac{\theta-\theta_0}{k}$	$\frac{1}{k}\log\frac{\sin\theta}{\sin\theta_0}$	$\frac{1}{k}\log\frac{1}{1-kv_0t_v}$	$\frac{2\cos\theta_0}{kv_0}$	$\frac{1}{k}(\pi-2\theta_0)$	$\frac{1}{k}\log\csc\theta_0$
$v_1\tanh(Az+B)$	$\frac{\beta\sin\theta_0}{A(\beta^2\sin^2\theta_0-1)^{1/2}}\left[\tan^{-1}\left(\frac{\cos\theta_0}{(\beta^2\sin^2\theta_0-1)^{1/2}}\right)-\tan^{-1}\left(\frac{\cos\theta}{(\beta^2\sin^2\theta_0-1)^{1/2}}\right)\right]$, $\beta=\frac{v_1}{v_0}$	$\frac{1}{A}\left[\tanh^{-1}\left(\frac{\sin\theta}{\beta\sin\theta_0}\right)-B\right]$, $\beta=\frac{v_1}{v_0}$	$\frac{1}{A}[\sinh^{-1}(e^{Av_1t_v}\sinh B)-B]$	$\frac{2}{Av_1(\beta^2\sin^2\theta_0-1)^{1/2}}\tan^{-1}\frac{\cos\theta_0}{(\beta^2\sin^2\theta_0-1)^{1/2}}+\frac{2}{Av_1}\tanh^{-1}\cos\theta_0$, $\beta=\frac{v_1}{v_0}$	$\frac{2\beta\sin\theta_0}{A(\beta^2\sin^2\theta_0-1)^{1/2}}\tan^{-1}\frac{\cos\theta_0}{(\beta^2\sin^2\theta_0-1)^{1/2}}$, $\beta=\frac{v_1}{v_0}$	$\frac{1}{A}[\coth^{-1}(\beta\sin\theta_0)-B]$, $\beta=\frac{v_1}{v_0}$
$v_1-\frac{A}{z+a}$	$\frac{A\sin\theta_0}{v_0(\beta^2\sin^2\theta_0-1)}\left\{\beta\sin\theta_0\left[\frac{\cos\theta_0}{(\beta-1)\sin\theta_0}-\frac{\cos\theta}{\beta\sin\theta_0-\sin\theta}\right]+\frac{1}{(\beta^2\sin^2\theta_0-1)^{1/2}}\left[\sin^{-1}\left(\frac{\beta\sin\theta_0\sin\theta-1}{\beta\sin\theta_0-\sin\theta}\right)-\sin^{-1}\left(\frac{\beta\sin^2\theta_0-1}{(\beta-1)\sin\theta_0}\right)\right]\right\}$, $\beta=\frac{v_1}{v_0}$	$\frac{a(\sin\theta-\sin\theta_0)}{\beta\sin\theta_0-\sin\theta}$, $\beta=\frac{v_1}{v_0}$	$t_v=\frac{1}{v_1}\left[z+\frac{A}{v_1}\log\left(1+\frac{\beta z}{a}\right)\right]$, $\beta=\frac{v_1}{v_0}$	$\frac{2a(\beta-1)}{\beta^2v_0}\left\{\log\cot\frac{\theta_0}{2}+\frac{\beta\cos\theta_0}{(\beta-1)(\beta^2\sin^2\theta_0-1)}+\frac{2\beta^2\sin^2\theta_0-1}{(\beta^2\sin^2\theta_0-1)^{3/2}}\left[\frac{\pi}{2}-\sin^{-1}\frac{\beta\sin^2\theta_0-1}{(\beta-1)\sin\theta_0}\right]\right\}$, $\beta=\frac{v_1}{v_0}$	$\frac{2a(\beta-1)\sin\theta_0}{\beta^2\sin^2\theta_0-1}\left\{\frac{\beta\cos\theta_0}{\beta-1}+\frac{1}{(\beta^2\sin^2\theta_0-1)^{1/2}}\left[\frac{\pi}{2}-\sin^{-1}\frac{\beta\sin^2\theta_0-1}{(\beta-1)\sin\theta_0}\right]\right\}$, $\beta=\frac{v_1}{v_0}$	$\frac{a(1-\sin\theta_0)}{\beta\sin\theta_0-1}$, $\beta=\frac{v_1}{v_0}$
$v_1\left(1-\frac{z^2}{z_1^2}\right)^{-1/2}$	$z_1\sin\theta_0\left[\frac{\pi}{2}-\sin^{-1}\left(\frac{\cot\theta}{\cot\theta_0}\right)\right]$	$z_1(1-\sin^2\theta_0\csc^2\theta)^{1/2}$	$t_v=\frac{1}{2v_1z_1}\left[z(z_1^2-z^2)^{1/2}+z_1^2\sin^{-1}\left(\frac{z}{z_1}\right)\right]$	$\frac{\pi z_1}{2v_0}(1+\sin^2\theta_0)$	$\pi z_1\sin\theta_0$	$z_1\cos\theta_0$
$v_0(1+A^2z^2)^{1/2}$	$\frac{1}{A\sin\theta_0}\left[E\left(\frac{\pi}{2},\cos\theta_0\right)-E(\psi,\cos\theta_0)\right]$, $\psi=\sin^{-1}(\sec\theta_0\cos\theta)$	$\frac{1}{A}(\sin^2\theta\csc^2\theta_0-1)^{1/2}$	$\frac{1}{A}\sinh Av_0t_v$	$\frac{2}{Av_0}K(\cos\theta_0)$	$\frac{2}{A\sin\theta_0}E\left(\frac{\pi}{2},\cos\theta_0\right)$	$\frac{1}{A}\cot\theta_0$
$A\left(\frac{z}{z+h}\right)^{1/2}$	$\frac{hp^2A^2\sin\theta\cos\theta}{(p^2A^2-\sin^2\theta)(1-p^2A^2)}+\frac{hpA}{2(p^2A^2-1)^{3/2}}\left[\frac{\pi}{2}-\sin^{-1}\left(\frac{p^2A^2-(2p^2A^2-1)\sin^2\theta}{p^2A^2-\sin^2\theta}\right)\right]$	$\frac{h\sin^2\theta}{p^2A^2-\sin^2\theta}$	$t_v=\frac{1}{A}\left\{[z(z+h)]^{1/2}+h\tanh^{-1}\left(\frac{z}{z+h}\right)^{1/2}\right\}$	$\frac{\pi h(2p^2A^2-1)}{A(p^2A^2-1)^{3/2}}$	$\frac{\pi pAh}{(p^2A^2-1)^{3/2}}$	$\frac{h}{p^2A^2-1}$
$v_0\cosh Az$	$\frac{1}{A}\left[\frac{\pi}{2}-\sin^{-1}\left(\frac{\cos\theta}{\cos\theta_0}\right)\right]$	$\frac{1}{A}\cosh^{-1}\left(\frac{\sin\theta}{\sin\theta_0}\right)$	$\frac{1}{A}\sinh^{-1}(\tan v_0At_v)$	$\frac{\pi}{v_0A}$	$\frac{\pi}{A}$	$\frac{1}{A}\cosh^{-1}(\csc\theta_0)$

TABLE II

RELATIONS BASED ON A GIVEN INSTANTANEOUS-VELOCITY—VERTICAL-TIME FUNCTION

Instantaneous-Velocity—Vertical-Time Function	Corresponding Average-Velocity—Vertical-Time Function	Corresponding Instantaneous-Velocity—Depth Function	Corresponding Average-Velocity—Depth Function	Travel Time from Shot-point to any Point of Path	Displacement	Vertical Depth to any Point of Path	Depth—Vertical-Time Function	Surface-to-Surface Travel Time	Range	Depth to Maximum Penetration
$v=v(t_v)$	$v_a=v_a(t_v)$	$v=v(z)$	$v_a=v_a(z)$	$t(\theta)$	$x(\theta)$	$z(\theta)$	$z=z(t_v)$	T	X	Z
$v_0(1+Kt_v)^{1/n}$	$\frac{nv_0}{(n+1)K}\cdot\frac{(1+Kt_v)^{(n+1)/n}-1}{t_v}$	$v_0\left(1+\frac{K(n+1)}{nv_0}z\right)^{1/(n+1)}$	$\frac{Kz}{\left(1+\frac{K(n+1)}{nv_0}z\right)^{n/(n+1)}-1}$	$\frac{n}{K\sin^n\theta_0}\int_{\theta_0}^{\theta}\sin^{n-1}\theta\,d\theta$	$\frac{nv_0}{K\sin^{n+1}\theta_0}\int_{\theta_0}^{\theta}\sin^{n+1}\theta\,d\theta$	$\frac{nv_0}{(n+1)K}\left(\frac{\sin^{n+1}\theta}{\sin^{n+1}\theta_0}-1\right)$	$\frac{nv_0}{(n+1)K}[(1+Kt_v)^{(n+1)/n}-1]$	$\frac{2n}{K\sin^n\theta_0}\int_{\theta_0}^{\pi/2}\sin^{n-1}\theta\,d\theta$	$\frac{2nv_0}{K\sin^{n+1}\theta_0}\int_{\theta_0}^{\pi/2}\sin^{n+1}\theta\,d\theta$	$\frac{nv_0}{(n+1)K}(\csc^{n+1}\theta_0-1)$
$v_0+Bt_v^{1/n}$	$v_0+\frac{nB}{n+1}t_v^{1/n}$	$z=\left(\frac{v-v_0}{B}\right)^n\left(\frac{nv+v_0}{n+1}\right)$	$z=v_a\left[\frac{(n+1)(v_a-v_0)}{nB}\right]^n$	$\frac{nv_0^n}{B^n\sin^n\theta_0}\int_{\theta_0}^{\theta}(\sin\theta-\sin\theta_0)^{n-1}d\theta$	$\frac{nv_0^{n+1}}{B^n\sin^{n+1}\theta_0}\int_{\theta_0}^{\theta}\sin\theta(\sin\theta-\sin\theta_0)^{n-1}d\theta$	$\frac{v_0^{n+1}}{(n+1)B^n\sin^{n+1}\theta_0}(\sin\theta-\sin\theta_0)^n(n\sin\theta+\sin\theta_0)$	$t_v\left(v_0+\frac{nB}{n+1}t_v^{1/n}\right)$	$\frac{2nv_0^n}{B^n\sin^n\theta_0}\int_{\theta_0}^{\pi/2}(\sin\theta-\sin\theta_0)^{n-1}d\theta$	$\frac{2nv_0^{n+1}}{B^n\sin^{n+1}\theta_0}\int_{\theta_0}^{\pi/2}\sin\theta(\sin\theta-\sin\theta_0)^{n-1}d\theta$	$\frac{v_0^{n+1}}{(n+1)B^n\sin^{n+1}\theta_0}(1-\sin\theta_0)^n(n+\sin\theta_0)$
$v_0+Bt_v^{1/2}$	$v_0+\frac{2}{3}Bt_v^{1/2}$	$z=\frac{1}{3B^2}(v-v_0)^2(2v+v_0)$	$z=v_a\left[\frac{3(v_a-v_0)}{2B}\right]^2$	$\frac{2v_0^2}{B^2\sin^2\theta_0}[\cos\theta_0-\cos\theta-(\theta-\theta_0)\sin\theta_0]$	$\frac{2v_0^3}{B^2\sin^3\theta_0}\left\{(\cos\theta-\cos^2\theta_0)-(\cos\theta-\cos\theta_0)-\frac{\sin\theta_0}{2}\left[\theta-\theta_0-\frac{1}{2}\sin 2\theta+\frac{1}{2}\sin 2\theta_0\right]\right\}$	$\frac{v_0^3}{3B^2\sin^3\theta_0}(2\sin^3\theta+\sin^3\theta_0-3\sin^2\theta\sin\theta_0)$	$t_v\left(v_0+\frac{2B}{3}t_v^{1/2}\right)$	$\frac{4v_0^2}{B^2\sin^2\theta_0}\left[\cos\theta_0-\left(\frac{\pi}{2}-\theta_0\right)\sin\theta_0\right]$	$\frac{v_0^3}{B^2\sin^3\theta_0}[4\sin\theta_0-4\cos^2\theta_0+\sin\theta_0(2\theta_0-\sin 2\theta_0-\pi)]$	$\frac{v_0^3}{3B^2\sin^3\theta_0}(1-\sin\theta_0)^2(2+\sin\theta_0)$
$v_0e^{At_v}$	$\frac{v_0(e^{At_v}-1)}{At_v}$	v_0+Az	$\frac{Az}{\log\left(1+\frac{Az}{v_0}\right)}$	$\frac{1}{A}\log\frac{\tan(\theta/2)}{\tan(\theta_0/2)}$	$\frac{v_0}{A\sin\theta_0}(\cos\theta_0-\cos\theta)$	$\frac{v_0}{A}\left(\frac{\sin\theta}{\sin\theta_0}-1\right)$	$\frac{v_0}{A}(e^{At_v}-1)$	$\frac{2}{A}\log\cot\frac{\theta_0}{2}$	$\frac{2v_0}{A}\cot\theta_0$	$\frac{v_0}{A}(\csc\theta_0-1)$